Journal of Materials Chemistry C

Accepted Manuscript

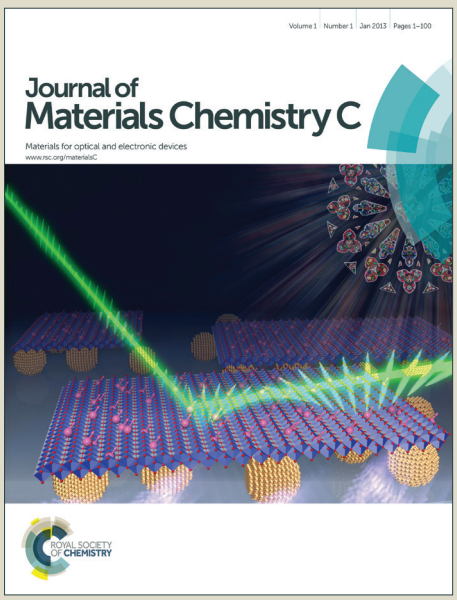

ROYAL SOCIETY OF CHEMISTRY

www.rsc.org/materialsC

Journal of Materials Chemistry C

Cite this: DOI: 10.1039/c0xx00000x

www.rsc.org/xxxxxx

ARTICLE TYPE

Highly sensitive conjugated polymer fluorescent sensors based on benzochalcogendiazole for nickel ions in real-time detection

Yunxiang Lei, Hui Li, Wenxia Gao, Miaochang Liu, Jiuxi Chen, Jinchang Ding, Xiaobo Huang* and Huayue Wu*

Received (in XXX, XXX) Xth XXXXXXXXX 20XX, Accepted Xth XXXXXXXXX 20XX

DOI: 10.1039/b000000x

Reports about fluorescent sensors for the highly sensitive and selective detection of Ni^{2+} are rare compared with Hg^{2+}, Ag^{+}, Cd^{2+}, Pb^{2+} and Cr^{3+} etc. Herein, we report the synthesis and application of two conjugated polymer fluorescent sensors, **P-1** and **P-2**, using benzochalcogendiazole and triazole as cooperative receptors of Ni^{2+}. The synthesis was carried out by the polymerization of 4,7-diethynylbenzoselenadiazole (**M-2**) and 4,7-diethynylbenzothiadiazole (**M-3**) with 2,7-diazido-9,9-dioctyl-9*H*-fluorene (**M-1**) *via* copper-catalyzed azide-alkyne cycloaddition. **P-1** and **P-2** exhibit emission peaks at 535 nm and 514 nm, and show yellow and green fluorescence, respectively. These two polymers showed outstanding fluorescence response behavior toward Ni^{2+} during real-time detection. Compared with benzothiadiazole-based **P-2**, benzoselenadiazole-based **P-1** showed higher sensitivity and selectivity and its detection limit could reach 2.4 nM, which might be due to the specific electronegativity of selenium. This work increases the application scope of the click reaction in regard to the design and synthesis of novel conjugated polymer fluorescence sensors based on the benzochalcogendiazole unit.

Introduction

Over the last two decades, conjugated polymer fluorescent sensors for heavy and transition metal (**HTM**) ions, anions, and organic molecules have attracted much interest owing to their high sensitivity, selectivity, rapidity and ease of measurement.[1] Their excellent sensitivity is attributed to sensory signal amplification that originates from energy migration along the conjugated backbone upon light excitation, and this was pointed out by Swager and coworkers.[2] Ni^{2+} is a dangerous and widespread global pollutant[3] but reports concerning fluorescence sensors for Ni^{2+} detection are still relatively scarce compared with Hg^{2+}, Ag^{+}, Cd^{2+}, Pb^{2+} and Cr^{3+} etc.[4] Ni^{2+}-sensitive fluorescent sensors are often based on small molecules and some have serious interference problems from other **HTM** ions like Cu^{2+}, Pb^{2+}, Co^{2+}, Hg^{2+}, Zn^{2+} and Fe^{2+} etc.[5] Very few fluorescence sensors based on conjugated polymers for Ni^{2+} detection have been reported,[6] and they often show unsatisfactory selectivity because their structures mostly incorporate bipyridyl or oligopyridyl groups, which exhibit a strong ability to coordinate with several metal ions. The development of highly selective and sensitive conjugated polymer fluorescence sensors for the detection of Ni^{2+} remains a challenge for researchers.

Recently, the copper-catalyzed azide-alkyne cycloaddition reaction (CuAAC) has had an enormous impact on the field of polymer material science because of its high efficiency, mild reaction conditions and technical simplicity.[7] In the click reaction, a thiazole ring is directly generated. The click-formed triazole can be used as a metal-binding ligand and it is more than a simple linker group. Many fluorescent sensors based on a triazole unit exist for metal ion detection.[8] However, these fluorescent sensors are mostly based on small organic molecules,[8,9] and only a few are based on conjugated polymers.[6e,10]

Benzochalcogendiazoles, such as 2,1,3-benzothiadiazole (**BT**) and 2,1,3-benzoselenadiazole (**BSe**), play very important roles in the synthesis and application of π-conjugated structure fluorescent sensors because they are excellent fluorophores owing to their strong and stable fluorescence, good thermal stability and good electron-withdrawing ability.[11] Comparisons between the effects of the heteroatoms S and Se are common since Se is much larger and less electronegative than S. It has been reported that **BSe**-based compounds have obvious absorption and emission redshifts compared with **BT**-based compounds because **BSe** can more effectively lower band gaps, and some of these compounds exhibit interesting photoelectric properties.[12] Additionally, benzochalcogendiazole units containing C=N bonds can also be used as recognition moieties and display high affinity toward transition metal ions.[13]

In this work, we report the synthesis and application of two new conjugated polymer fluorescent sensors, **P-1** and **P-2**, which

incorporate a benzochalcogendiazole unit and a triazole unit by the polymerization of 4,7-diethynylbenzoselenadiazole (**M-2**) and 4,7-diethynylbenzothiadiazole (**M-3**) with 2,7-diazido-9,9-dioctyl-9*H*-fluorene (**M-1)** *via* the CuAAC reaction, respectively. Both these two polymers are soluble in common organic solvents and highly emissive. The sensing properties of these two polymers were investigated using benzochalcogendiazole and triazole as cooperative receptors for metal ions by obtaining fluorescence spectra for real-time detection. Although both these polymers were highly sensitive toward Ni^{2+}, compared with **P-2** based on **BT**, **P-1** based on **BSe** showed higher sensitivity and selectivity because of the specific electronegativity of selenium.

Experimental section

Measurements and materials

^{1}H NMR and ^{13}C NMR spectra were recorded as $CDCl_3$ solutions on a Bruker DRX 500 NMR spectrometer with tetramethylsilane (TMS) as the internal standard. The chemical shift was recorded in ppm and the following abbreviations were used to indicate multiplicities: s = singlet, d = doublet, m = multiplet, br = broad. EI mass spectra were recorded on an Agilent 5975C DIP/MS mass spectrometer. C, H and N elemental analyses were performed on an Elementar Vario MICRO analyzer. UV-vis absorption was recorded on a Shimadzu UV-1700 spectrometer and fluorescence spectra were recorded on a RF-5301PC fluorometer. Thermogravimetric analysis (TGA) was performed on a Perkin-Elmer Pyris-1 instrument under a N_2 atmosphere. Molecular weight was determined by gel permeation chromatography (GPC) with a Waters-244 HPLC pump. THF was used as the solvent and the results are relative to polystyrene standards. THF and Et_3N were purified by distillation from sodium in the presence of benzophenone. The other solvents were commercially available and analytical reagent grade. The other materials were common commercial grade and used as received.

Preparation of monomer M-1

9,9-Dioctyl-9*H*-fluorene (**2**) was synthesized according to a reported method.[14] 1-Bromooctane (4.26 g, 22 mmol) was added using a syringe to a mixture of fluorene (**1**) (1.66 g, 10.0 mmol) and KOH (5.6 g, 100 mmol) in THF (25 mL) at room temperature. The reaction mixture was stirred at room temperature for 12 h. Upon evaporation to dryness, the residue was extracted with $CHCl_3$ and washed with water and then brine, dried over anhydrous Na_2SO_4, and then evaporated under vacuum to dryness. The residue was purified by silica gel column chromatography (petroleum ether/ethyl acetate) (200:1, v/v) to give compound **2** as a yellow oil in 82% yield.

2,7-Dinitro-9,9-dioctyl-9*H*-fluorene (**3**) was synthesized according to a reported method.[15] Compound **2** (5 g, 12.8 mmol) was dissolved in 10 mL glacial acetic acid in a round-bottom flask. The solution was chilled to 0 °C and then 10 mL fuming nitric acid was added dropwise. The reaction mixture was allowed to warm to room temperature and then it was stirred for 2 h. The reaction mixture was poured on ice and then extracted with $CHCl_3$. The organic layer was washed with water, saturated $NaHCO_3$ solution, and then brine, dried over anhydrous Na_2SO_4, and then evaporated under vacuum to dryness. The residue was purified by silica gel column chromatography (petroleum ether/CH_2Cl_2) (1:5, v/v) to give compound **3** as a yellow solid in 50% yield. ^{1}H NMR (500 MHz, $CDCl_3$): δ 8.33 (dd, J_1 = 8.5 Hz, J_2 = 2.0 Hz, 2H), 8.26 (d, J = 2.0 Hz, 2H), 7.93 (d, J = 8.5 Hz, 2H), 2.12–2.08 (m, 4H), 1.17–1.01 (m, 20H), 0.78 (t, J = 7.0 Hz, 6H), 0.58–0.52 (m, 4H); ^{13}C NMR (125 MHz, $CDCl_3$): δ 153.5, 148.4, 144.7, 123.5, 121.5, 118.5, 56.4, 39.7, 31.6, 29.7, 29.1, 29.0, 23.8, 22.5, 13.9.

9,9-Dioctyl-9*H*-fluorene-2,7-diamine (**4**) was synthesized according to a reported method.[16] A mixture of compound **3** (0.50 g, 1.2 mmol), zinc powder (2.00 g), anhydrous $CaCl_2$ (0.30 g), ethanol (30 mL) and water (10 mL) was refluxed for 5 h, and then the hot mixture was filtered to remove the zinc powder. The mixture was extracted with $CHCl_3$, and the organic layer was washed with water and brine, dried over anhydrous Na_2SO_4, and then evaporated under vacuum to dryness. The residue was purified by silica gel column chromatography (petroleum ether/ethyl acetate) (1:5, v/v) to give compound **4** as a yellow oil in 90% yield. ^{1}H NMR (500 MHz, $CDCl_3$): δ 7.35 (d, J = 8.0 Hz, 2H), 6.63 (s, 2H), 6.61 (d, J = 2.0 Hz, 2H), 3.64 (br, 4H), 1.86–1.83 (m, 4H), 1.25–1.06 (m, 20H), 0.85 (t, J = 7.0 Hz, 6H), 0.67 (br, 4H); ^{13}C NMR (125 MHz, $CDCl_3$): δ 151.6, 144.4, 133.1, 119.0, 113.8, 110.0, 54.6, 40.9, 31.8, 30.2, 29.3, 29.2, 23.7, 22.6, 14.0.

2,7-Diazido-9,9-dioctyl-9*H*-fluorene (**M-1**) was synthesized according to a reported method.[16] Compound **4** (0.4 g, 1.1 mmol) was dissolved in a mixture of 30 mL water and 10 mL concentrated hydrochloric acid in a round-bottom flask at 0 °C. Sodium nitrite (0.18 g, 2.3 mmol) was added dropwise to the above solution. After 1 h of stirring, sodium azide (0.16 g, 2.5 mmol) was added dropwise. The reaction mixture was stirred at 0 °C for 4 h. The mixture was extracted with CH_2Cl_2, and the organic layer was washed with water and brine, dried over anhydrous Na_2SO_4, and then evaporated under vacuum to dryness. The residue was purified by silica gel column chromatography eluting with petroleum ether to give **M-1** as a yellow solid in 93% yield. ^{1}H NMR (500 MHz, $CDCl_3$): δ 7.60 (d, J = 8.0 Hz, 2H), 7.00 (dd, J_1 = 8.0 Hz, J_2 = 2.0 Hz, 2H), 6.95 (d, J = 2.0 Hz, 2H), 1.94–1.90 (m, 4H), 1.23–1.04 (m, 20H), 0.83 (t, J = 7.5 Hz, 6H), 0.59–0.57 (m, 4H); ^{13}C NMR (125 MHz, $CDCl_3$): δ 152.6, 138.7, 137.6, 120.5, 117.9, 113.6, 55.4, 40.4, 31.7, 29.9, 29.2, 29.1, 23.6, 22.6, 14.0.

Synthesis of monomer M-2

3,6-Dibromobenzene-1,2-diamine (**7**) (532 mg, 2.0 mmol), $Pd(PPh_3)_2Cl_2$ (140.2 mg, 0.20 mmol), CuI (38.2 mg, 0.20 mmol), PPh_3 (52.4 mg, 0.20 mmol) and trimethyl silyl acetylene (1.72 mL, 12.00 mmol) were dissolved in a solvent mixture of Et_3N (25 mL) and THF (25 mL). The reaction mixture was stirred at 80 °C for 12 h under N_2. After cooling to room temperature, the solvent was removed using a rotary evaporator and the residue was extracted with $CHCl_3$. The organic extract was washed with water and then brine, dried over anhydrous Na_2SO_4, and then evaporated under vacuum to dryness. The residue was purified by silica gel column chromatography (petroleumether/ethyl acetate) (30:1, v/v) to give compound **8** as a yellow solid in 42% yield. MS (EI, m/z): 300 (M^+).

To a solution of compound **8** (112.2 mg, 0.38 mmol) in refluxing ethanol (40 mL) was added a solution of SeO_2 (43.2 mg, 0.4 mmol) in hot water (20 mL). The reaction mixture was stirred under reflux for 2 h. After cooling to room temperature, the solvent was removed using a rotary evaporator and the residue was extracted with $CHCl_3$. The organic layer was washed with water and then brine, dried over anhydrous Na_2SO_4, and then evaporated under vacuum to dryness. The residue was purified by silica gel column chromatography using petroleum ether as an eluent to give compound **9** as a yellow solid in 75% yield. ^{1}H NMR (500 MHz, $CDCl_3$): δ 7.62 (s, 2H), 0.33 (s, 18H); ^{13}C NMR (125 MHz, $CDCl_3$): δ 158.0, 132.8, 118.2, 102.3, 99.5, -1.2.

Compound **9** (100 mg, 0.26 mmol) was dissolved in a mixed solvent of THF (20 mL) and MeOH (20 mL), and then K_2CO_3 (26 mg, 0.266 mmol) was added to the solution. The reaction mixture was stirred at room temperature for 1 h. The solvent was removed under reduced pressure and the residue was extracted with $CHCl_3$. The organic layer was washed with water and then brine, dried over anhydrous Na_2SO_4 and then evaporated under vacuum to dryness to give the yellow solid **M-2** in 82% yield. ^{1}H NMR (500 MHz, $CDCl_3$): δ 7.66 (s, 2H), 3.67 (s, 2H); ^{13}C NMR (125 MHz, $CDCl_3$): δ 159.1, 133.4, 118.5, 85.2, 79.4.

Synthesis of monomer M-3

4,7-Diethynylbenzothiadiazole (**M-3**) was synthesized as previously reported.[11c,17] 4,7-Dibromobenzothiadiazole (**6**) (1.10 g, 3.75 mmol), $Pd(PPh_3)_4$ (87.5 mg, 0.075 mmol), CuI (27.5 mg, 0.15 mmol) and trimethylsilyl acetylene (1.5 mL, 11.25 mmol) were dissolved in 50 mL Et_3N. The reaction mixture was stirred at 75 °C for 5 h under N_2. After cooling to room temperature, the solvent was removed by rotary evaporation and the residue was extracted with CH_2Cl_2 (2 × 30 mL). The combined organic layers were washed with water and 1.2 mol·L^{-1} HCl (30 mL), and then dried over anhydrous Na_2SO_4. Upon evaporation to dryness, the residue was purified by silica gel column chromatography using petroleum ether/ethyl acetate (15:1, v/v) as an eluent to give compound **10** as a pale yellow solid in 95% yield. Compound **10** was directly used for the synthesis of **M-3** without further purification.

Compound **10** (450 mg, 1.35 mmol) in a KOH methanol solution (1 mol·L^{-1}, 35 mL) was stirred at room temperature for 1 h. The solvent was removed under reduced pressure and the residue was extracted with $CHCl_3$. The organic layer was washed with water and then brine, dried over anhydrous Na_2SO_4, and then evaporated under vacuum to dryness to give **M-3** as a yellow solid in 90% yield. ^{1}H NMR (500 MHz, $CDCl_3$): δ 7.75 (s, 2H), 3.67 (s, 2H); ^{13}C NMR (125 MHz, $CDCl_3$): δ 154.3, 133.2, 116.7, 85.3, 78.9.

Preparation of the conjugated polymers P-1 and P-2

A mixture of **M-1** (118.2 mg, 0.25 mmol), **M-2** (57.8 mg, 0.25 mmol), 10 mol% sodium ascorbate (4.95 mg, 0.025 mmol) and 5 mol% $CuSO_4·5H_2O$ (3.12 mg, 0.0125 mmol) was dissolved in a 10 mL THF, 2 mL *t*-BuOH and 2 mL H_2O solvent mixture. The reaction mixture was stirred at 30–36 °C for 2 d under N_2. The solvents were removed under reduced pressure and the residue was extracted with $CHCl_3$ (3 × 50 mL). The combined organic layers were washed with an aqueous NH_4OH solution, water and then dried over anhydrous Na_2SO_4. After the solution was removed, the resulting polymer was precipitated in methanol, and then filtered and washed with methanol several times. Further purification was conducted by dissolving the polymer in $CHCl_3$ to precipitate in methanol. The polymer was dried under vacuum to give 120.0 mg **P-1** as an orange solid in 57.8% yield. GPC results: M_w = 7560, M_n = 5880, PDI = 1.29. ^{1}H NMR (500 Hz, $CDCl_3$): δ 9.26 (br, 2H), 8.76–7.58 (m, 6H), 7.05–6.94 (m, 2H), 2.02–1.91 (m, 4H), 1.25-1.08 (m, 20H), 0.79–0.64 (m, 10H). FT-IR (KBr, cm^{-1}): 2926, 2851, 1610, 1582, 1465. Anal. calcd for $C_{39}H_{44}N_8Se$: C, 66.56; H, 6.30; N, 15.92. Found: C, 63.45; H, 6.01; N, 13.49.

Using the same procedure as for the preparation of **P-1**, **P-2** was obtained as a brown solid in 75.5% yield from **M-3** and **M-1**. GPC results: M_w = 9400, M_n = 7200, PDI = 1.31. **P-2** spectroscopic data: ^{1}H NMR (500 Hz, $CDCl_3$): δ 9.29–9.25 (m, 2H), 8.84–7.71 (m, 6H), 7.06–7.02 (m, 2H), 2.18–2.01 (m, 4H), 1.25-1.11 (m, 20H), 0.79–0.66 (m, 10H). FT-IR (KBr, cm^{-1}): 2924, 2852, 1610, 1588, 1475. Anal. calcd for $C_{39}H_{44}N_8S$: C, 71.31; H, 6.75; N, 17.06. Found: C, 68.56; H, 6.21; N, 15.32.

Metal ion titrations with P-1 and P-2

Each metal ion titration experiment was started using 3.0 mL polymer fluorescent sensor in a $CHCl_3$ solution of known concentration (10 μmol·L^{-1}). Mercury perchlorate salt and various other metal salts (nitrates) in CH_3CN were used for the titration. Because the minimum response time that can be measured is limited by the manipulation time, all measurements were obtained 10 s after the addition of the metal salt to the polymer solutions for real-time detection.

Results and Discussion

Synthesis and features of the conjugated polymers

The synthesis procedures of the monomers **M-1**, **M-2** and **M-3** and the conjugated polymers **P-1** and **P-2** are outlined in **Scheme 1**. Monomer **M-1** was synthesized from fluorene (**1**) in a five-step reaction as reported previously.[11-16] Monomers **M-2**[18] and **M-3**[11c,17] were synthesized from benzothiadiazole (**5**) in a three-step reaction and five-step reaction as reported previously, respectively. The terminal alkynes **M-2** and **M-3** are unstable and need to be kept in the dark and under a N_2 atmosphere at -4 °C before use.

M-1, **M-2** and **M-3** were used as monomers for the synthesis of the target polymers. We used a typical click reaction for the synthesis of these polymers.[10a,19] The polymerization was carried out under mild reaction conditions in a THF/*t*-BuOH/H_2O solution in the presence of a catalytic amount of sodium ascorbate (10 mol%) and $CuSO_4·5H_2O$ (5 mol%). The number-average molecular weight (M_n) was determined to be 5880 for **P-1** and 7200 for **P-2** by GPC using a polystyrene standard in THF. The GPC results of these two polymers show a moderate molecular weight. The resulting polymers show good solubility in common solvents including $CHCl_3$, CH_2Cl_2, toluene and THF, and this can be attributed to the flexible *n*-octyl group on the fluorene units,

Cite this: DOI: 10.1039/c0xx00000x

www.rsc.org/xxxxxx

ARTICLE TYPE

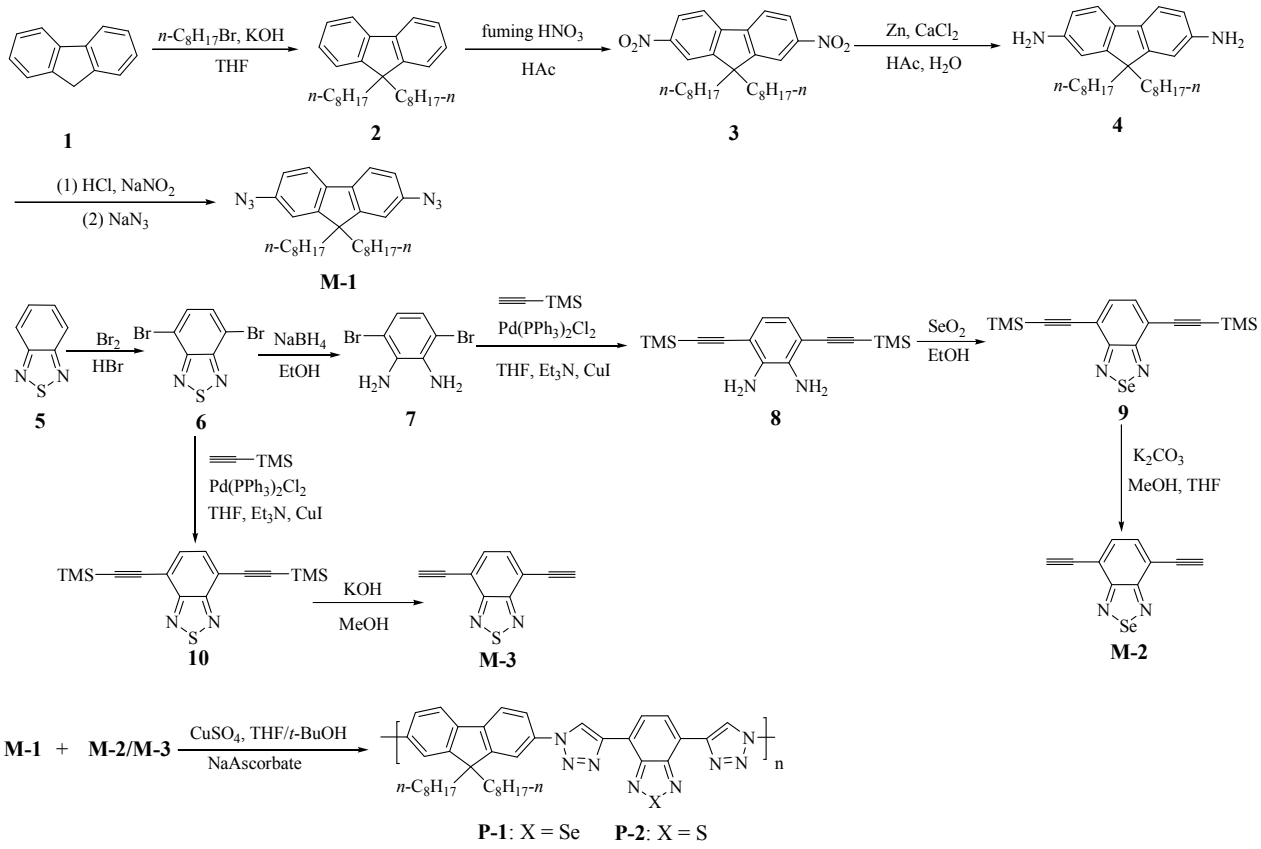

Scheme 1 Synthetic routes to **M-1**, **M-2**, **M-3** and the conjugated polymers **P-1** and **P-2**.

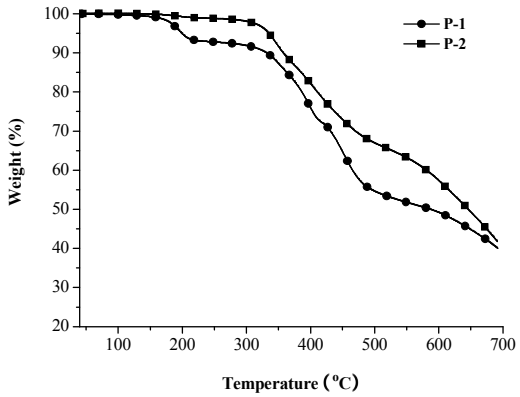

Fig. 1 TGA curves of **P-1** and **P-2**.

which are side chains on the polymers. The TGA of the polymers was carried out under a N_2 atmosphere at a heating rate of 10 °C/min (**Fig. 1**). As shown in **Fig. 1**, although the **P-1** and **P-2** repeating units have a similar polymer composition and backbone chain structure, their TGA plots are different. The TGA curves reveal that the 5% weight loss temperatures (T_d) for **P-1** and **P-2** are 211 °C and 334 °C, respectively. There is a total loss of about 60% and 58% for **P-1** and **P-2** when heated to 700 °C, respectively. By comparison with **P-1**, **P-2** has higher stability, which can be ascribed to the high thermal stability of the **BT** unit. These results indicate that these two polymers have a desirable thermal property for use in fluorescent materials.

Optical properties

The UV-vis absorption and fluorescence spectra of **P-1** and **P-2** were recorded in $CHCl_3$ as shown in **Fig. 2**. As is evident from **Fig. 2**, these two polymers exhibit two distinct absorption bands in the range of 300 nm to 500 nm. The band in the shorter wavelength 300–350 nm region is assigned to a localized π-π*

transition, and the other band at around 360–500 nm is assigned to the effective π electronic transition of the conjugated units in the main-chain backbone.[12e] **P-1** and **P-2** exhibit emission peaks at 535 nm and 514 nm, and show yellow and green fluorescence, respectively. A red shift (21 nm) was observed for the fluorescence spectra of **P-1** by comparison with that of **P-2**, which is related to the narrower π-π* gap of the aromatic Se-containing heterocycle.[12a] The fluorescence quantum yields (Φ_F) of these two polymers were determined in $CHCl_3$ at room temperature using the quinine sulfate solution as a fluorescence reference (Φ_r = 0.55 in 0.5 mol/L H_2SO_4). The Φ_F values could be calculated using the equation: $\Phi_F = \Phi_r (F_s/F_r)(A_r/A_s)(\eta_s/\eta_r)^2$, where s and r denote the sample and reference, respectively, F is the integrated fluorescence intensity, A is the absorbance at the excited wavelength, and η is the refractive index of the solvent.[20] **P-1** based on **BSe** has low fluorescence quantum yield (Φ_F = 0.13) compared with **P-2** based on **BT** polymer (Φ_F = 0.27), and the result is similiar to those previously reported,[12m,18] which could be due to the fact that the narrow energy bandgap may increase the probability of singlet excitons decaying to the ground state in a nonradiative way.[12m]

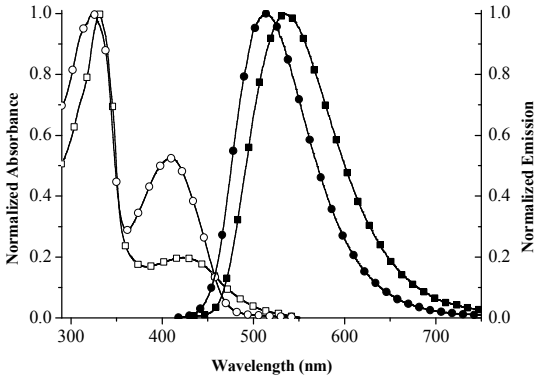

Fig. 2 Absorption spectra of **P-1 (-□-)** and **P-2 (-○-)**, and fluorescence spectra of **P-1 (-■-,** λ_{ex} = 425 nm**)** and **P-2 (-●-,** λ_{ex} = 408 nm**)** in $CHCl_3$.

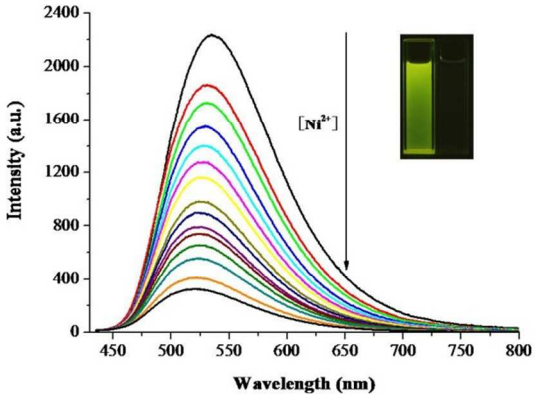

Fig. 3 Fluorescence spectra of **P-1** (10.0 μmol L^{-1} in $CHCl_3$) with increasing concentrations of Ni^{2+} (0, 0.2, 0.4, 0.6, 0.8, 1, 1.2, 1.4, 1.6, 1.8, 2.0, 2.5, 3.0, 4.0, 5.0 μmol·L^{-1} in CH_3CN) (λ_{ex} = 425 nm). Inset: Visible fluorescence of **P-1** before (left) and after (right) the addition of Ni^{2+} (5.0 μmol·L^{-1}) under a 365 nm UV lamp.

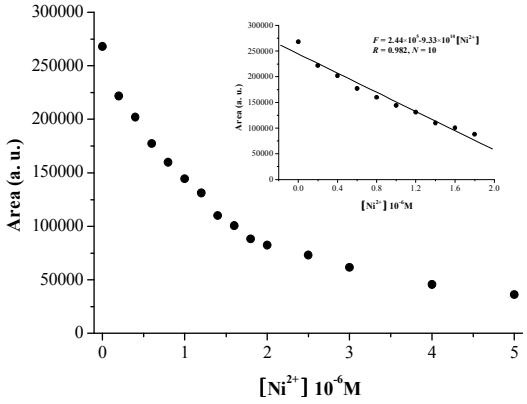

Fig. 4 Calibration curve obtained from a plot of the fluorescence intensity of **P-1** with added Ni^{2+} from 0 to 5.0 μmol·L^{-1}. Inset: linear plot obtained at low concentrations of Ni^{2+} (0 to 1.8 μmol·L^{-1}).

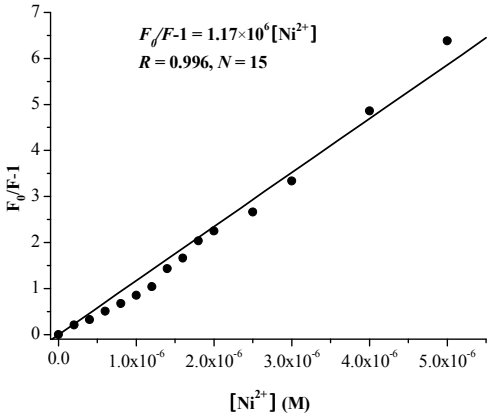

Fig. 5 Stern-Volmer plot of **P-1** emission upon quenching by Ni^{2+} (0 to 5.0 μmol·L^{-1}).

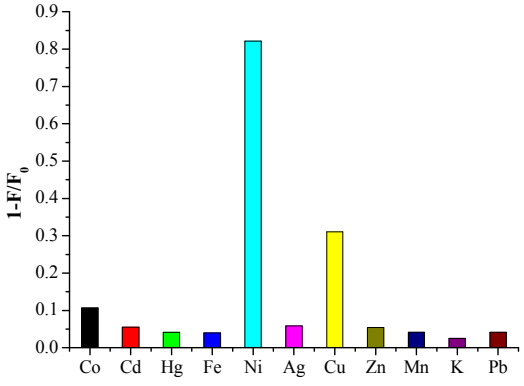

Fig. 6 Relative fluorescence quenching of **P-1** (10.0 μmol·L^{-1}) in the presence of various metal ions (each 4.0 μmol·L^{-1}).

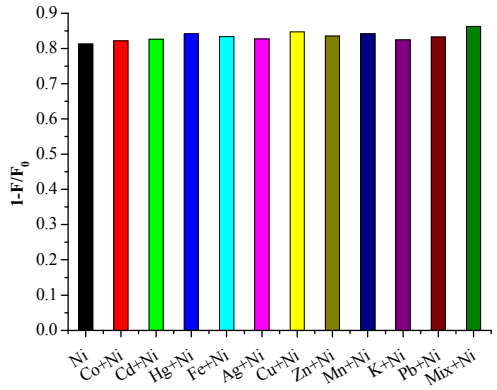

Fig. 7 Metal specificity: the concentration of **P-1** was 10.0 μmol·L^{-1}. The concentration of Ni^{2+} and the other metal ions was 4.0 μmol·L^{-1}. Mix: mixture of Co^{2+}, Cd^{2+}, Hg^{2+}, Fe^{3+}, Ag^{+}, Cu^{2+}, Zn^{2+}, Mn^{2+}, K^{+} and Pb^{2+}.

Fluorescence-sensing properties of P-1 and P-2 toward Ni^{2+}

We first investigated the UV-vis absorption response behaviors of **P-1** and **P-2** (see **Fig. S1** and **Fig. S2** in the ESI) in $CHCl_3$ toward various metal ions in CH_3CN, including K^{+}, Pb^{2+}, Cd^{2+}, Co^{2+}, Ag^{+}, Fe^{3+}, Hg^{2+}, Zn^{2+}, Ni^{2+}, Cu^{2+} and Mn^{2+}. Although the addition of some metal ions to the polymer solution could cause the changes of the UV-vis absorption spectra of **P-1** and **P-2**, these two polymers could not show outstanding response toward a specific metal ion. And so, in this work, we mainly studied the fluorescence-sensing properties of these two polymers for metal ions.

To provide a potential ‘‘zero-wait’’ detection method for metal ions, we first investigated the fluorescence-sensing properties of **P-1** upon the addition of various metal ions in real-time. All the measurements were obtained 10 s after the addition of the metal salt to the host molecule solutions. **Fig. 3** shows the fluorescence spectra of **P-1** (10.0 μmol·L^{-1} in $CHCl_3$) upon the addition of Ni^{2+} in CH_3CN upon excitation at 425 nm. Emission quenching upon the addition of Ni^{2+} was observed. The emission quenching may be attributed to energy or electron transfer between the metal complexes and the polymer backbone.[6b] The addition of Ni^{2+} led to 82.9% fluorescence quenching of **P-1** at a concentration of 4.0 μmol·L^{-1}. Additionally, the yellow **P-1** fluorescence disappeared after the addition of Ni^{2+}, and this was easily detected by the naked eye (**Fig. 3**, inset). Notably, the fluorescence intensity changed almost linearly with the concentration of Ni^{2+} in the range of 0–1.8 μmol·L^{-1}. The following curve equation was obtained: $F = 2.44\times10^{5}-9.33\times10^{10}[Ni^{2+}]$ (**Fig. 4**, inset), which indicates that Ni^{2+} can be quantitatively detected. According to this equation and the standard deviation of the blank, the fluorescence detection limit of **P-1** for Ni^{2+} was detemined to be 2.4 nM. The detection limit was sufficently low to detect the nanomolar concentrations of Ni^{2+} found in many chemical systems.

The fluorescence-quenching efficiency of the **P-1** sensor can be described by the Stern-Volmer equation: $F_0/F = 1 + K_{SV}[Q]$ and, herein, F_0 and F are the fluorescence intensities in the absence and presence of a quencher, respectively. K_{SV} is the quenching constant and $[Q]$ is the quencher concentration. At Ni^{2+} concentrations from 0 to 5.0 μmol·L^{-1}, a good linear Stern-Volmer plot of the fluorescence intensity of **P-1** versus the the concentrations of Ni^{2+} was obtained with a K_{SV} value of 1.17×10^{6} mol^{-1}·L, as shown in **Fig. 5**.

To determine the selectivity of the sensor toward Ni^{2+}, the fluorescence response behavior of **P-1** toward other important metal ions at a concentration of 4.0 μmol·L^{-1} was determined (**Fig. 6**). The degree of fluorescence quenching ($1-F/F_0$) of **P-1** was no more than 10% by the other metal ions including K^{+}, Pb^{2+}, Cd^{2+}, Co^{2+}, Ag^{+}, Fe^{3+}, Hg^{2+}, Zn^{2+} and Mn^{2+}. Fluorescence quenching of the **P-1** solution was observed upon the addition of Cu^{2+}, but the degree of fluorescence quenching (30%) was much smaller than that by Ni^{2+} ions. These results indicate that **P-1** shows good selectivity toward Ni^{2+} sensing compared with other ions. For effective Ni^{2+} detection, another essential requirement is that other metal ions exhibit no or little interference. Competition experiments were performed on the **P-1** solution in the presence of 4 μmol·L^{-1} of the other metal ions (**Fig. 7**). As shown in **Fig. 7**, the deviation in fluorescence quenching in the presence of the other metals ions was less than 6%. These results confirm the ability of **P-1** to sense Ni^{2+} with high selectivity even in the presence of other metal ions. The sensitivity and selectivity of **P-1** may be ascribed to the building block receptors from the **BSe** and triazole units in the main-chain backbone. These fit well, leading to the formation of a more stable Ni^{2+}-polymer complex compared with the other metal ions.

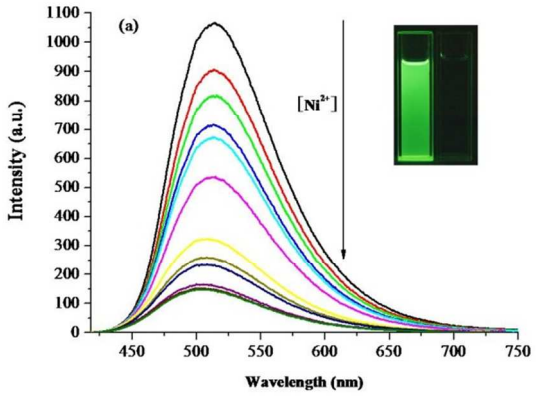

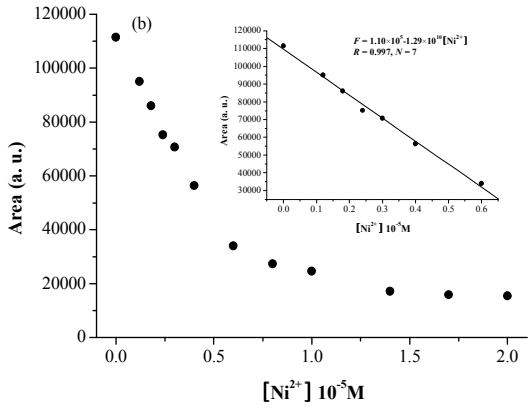

Fig. 8 (a) Fluorescence spectra of **P-2** (10.0 μmol L^{-1} in $CHCl_3$) with increasing concentrations of Ni^{2+} (0, 1.2, 1.8, 2.4, 3.0, 4.0, 6.0, 8.0, 10.0, 14.0, 17.0, 20.0 μmol·L^{-1} in CH_3CN) (λ_{ex} = 408 nm). Inset: Visible fluorescence of **P-2** before (left) and after (right) the addition of Ni^{2+} (20.0 μmol·L^{-1}) under a 365 nm UV lamp. (b) Fluorescence intensity of **P-2** versus Ni^{2+} concentration from 0 to 20.0 μmol·L^{-1}. Inset: linear plot obtained at low concentrations of Ni^{2+} (0 to 6.0 μmol·L^{-1}).

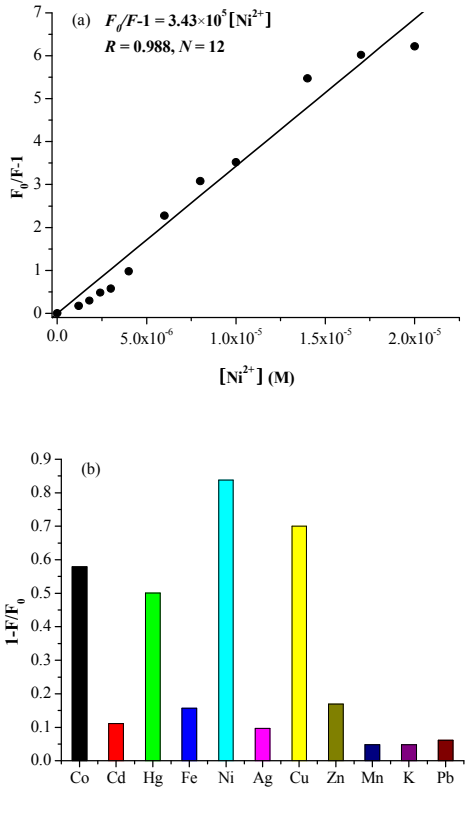

Fig. 9 (a) Stern-Volmer plot of **P-2** emission quenched by Ni^{2+} (0 to 20.0 μmol·L^{-1}). (b) Relative fluorescence quenching of **P-2** (10.0 μmol·L^{-1}) in the presence of various metal ions (each 14.0 μmol·L^{-1}).

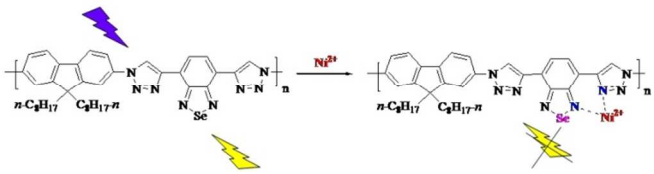

Fig. 10 Possible **P-1** nickel ion detection mechanism.

We also investigated the possible use of **P-2** for the determination of Ni^{2+} (**Fig. 8**). We found that Ni^{2+} resulted in 83.8% fluorescence quenching at a concentration of 14.0 μmol·L^{-1}. We obtained a linear equation for the fluorescence intensity of **P-2** *vs* Ni^{2+} concentration in the range of 0 to 6.0 μmol·L^{-1} Ni^{2+}: $F = 1.10\times10^5\text{-}1.29\times10^{10}[Ni^{2+}]$ (**Fig. 8b**, inset). The limit of detection was determined to be 11 nM. Furthermore, the K_{SV} value of **P-2** was calculated to be 3.43×10^5 mol^{-1}·L from the Stern-Volmer plot, as shown in **Fig. 9a**. Additionally, the results of the metal-binding properties of **P-2** toward the other metal ions showed that Co^{2+}, Hg^{2+} and Cu^{2+} could significantly quench **P-2** fluorescence, and the quenching ratios were 57.9, 50.0 and 70.0% at the same concentrations as those used for Ni^{2+}, respectively (**Fig. 9b**). According to these results, it can be concluded that **P-1** has higher sensitivity and selectivity toward Ni^{2+} detection than **P-2**.

The stoichiometry for Ni^{2+} with **P-1**/**P-2** can be determined on the basis of the Benesi-Hildebrand expression:[21] $1/(F\text{-}F_0) = 1/\{K(F_0\text{-}F_{min})[Ni^{2+}]^n\}\text{-}1/(F_0\text{-}F_{min})$, where F_{min} is the minimum fluorescence intensity in the presence of a quencher, and K is the associated constant. According to the fluorescence titration experiment data, the linear correlation coefficients of Benesi-Hildebrand plots for Ni^{2+}-bound **P-1** and Ni^{2+}-bound **P-2** (see **Fig. S3** and **Fig. S4** in the ESI) were 0.9958 and 0.9939 using the Benesi-Hildebrand equation of linear fitting based on 1:1 (n = 1), respectively. The results indicate that there is a 1:1 binding mode between **P-1**/**P-2** and Ni^{2+}. In addition, the associated constants obtained from the slope and intercept of the line were 2.03×10^6 mol^{-1}·L for **P-1** and 4.13×10^5 mol^{-1}·L for **P-2**. A possible mechanism for **P-1** nickel ion detection is shown in **Fig. 10**. We and others had reported several conjugated polymer fluorescent sensors for the selective detection of Hg^{2+} using benzochalcogendiazole or triazole as recognition unit, respectively, which indicate the individual **BT**[11a,b,e], **BSe**[11f] or triazole[6e,10] units tend to bind mercury ion. According to Bunz and coworkers,[13] a binding pocket for Ni^{2+} is formed between the nitrogen of the triazole and the nitrogen of the benzochalcogendiazole in the polymer backbone. The higher sensitivity and selectivity of **P-1** may be due to the lower electronegativity of selenium compared with sulfur, which is favorable for an adjustment of the aromaticity of the benzoselenadiazole cycle, the size of the binding pocket and the binding capacity of nitrogen, etc.[13]

Conclusions

Two conjugated polymer fluorescent sensors **P-1** and **P-2** using a benzochalcogendiazole unit and a triazole unit as cooperative

receptors were synthesized by the CuAAC reaction. The resulting polymers show good thermal stability and solubility in common organic solvents. **P-1** and **P-2** exhibit emission peaks at 535 nm and 514 nm and are characterized by yellow and green fluorescence, respectively. These two polymers show outstanding fluorescence response behavior toward Ni^{2+} in real-time detection and compared with **BT**-based **P-2**, the **BSe**-based **P-1** showed higher sensitivity and selectivity because of the specific electronegativity of selenium. The quenching of **P-1** fluorescence gave a linear response toward Ni^{2+} in the range of 0–1.8 μmol·L^{-1}, with a detection limit of 2.4 nM. The results indicate that **P-1** can be used as high sensitive and selective materials for the detection of Ni^{2+}. This study opens up new opportunities for the design of conjugated polymer fluorescence sensors based on the benzoselenadiazole unit.

Acknowledgements

This work was supported by the National Natural Science Foundation of China (No. 21204066), the Commonwealth Project of Science and Technology Department of Zhejiang Province (No. 2012C23030) and the Bureau of Science and Technology of Wenzhou (No. S20100007).

Notes and references

College of Chemistry & Materials Engineering, Wenzhou University, Wenzhou 325035, P. R. China.

E-mail:xiaobhuang@wzu.edu.cn; huayuewu@wzu.edu.cn

† Electronic Supplementary Information (ESI) available. See DOI: 10.1039/b000000x/

1 (a) D. T. McQuade, A. E. Pullen and T. M. Swager, *Chem. Rev.*, 2000, **100**, 2537-2574; (b) S. W. Thomas, G. D. Joly and T. M. Swager, *Chem. Rev.*, 2007, **107**, 1339-1386; (c) H. N. Kim, Z. Guo, W. Zhu, J. Yoon and H. Tian, *Chem. Soc. Rev.*, 2011, **40**, 79-93; (d) A. Alvarez, A. Salinas-Castillo, J. M. Costa-Fernández, R. Pereiro and A. Sanz-Medel, *Trend. Anal.Chem.*, 2011, **30**, 1513-1525; (e) L. J. Fan, Y. Zhang, C. B. Murphy, S. E. Angell, M. F. L. Parker, B. R. Flynn and W. E. Jones, *Coord. Chem. Rev.*, 2009, **253**, 410-422; (f) X. Feng, L. Liu, S. Wang and D. Zhu, *Chem. Soc. Rev.*, 2010, **39**, 2411-; (g) H. Shi, H. Sun, H. Yang, S. Liu, G. Jenkins, W. Feng, F. Li, Q. Zhao, B. Liu and W. Huang, *Adv. Funct. Mater.*, 2013, **23**, 3268-3276; (h) H. Shi, X. Chen, S. Liu, H. Xu, Z. An, L. Ouyang, Z. Tu, Q. Zhao, Q. Fan, L. Wang and W. Huang, *ACS Appl. Mater. Interfaces* 2013, **5**, 4562-4568; (i) H. Shi, S. Liu, Z. An, H. Yang, J. Geng, Q. Zhao, B. Liu and W. Huang, *Macromol. Biosci.* 2013, **13**, 1339-1346; (j) H. F. Shi, S. J. Liu, H. B. Sun, W. J. Xu, Z. F. An, J. Chen, S. Sun, X. M. Lu, Q. Zhao and W. Huang, *Chem. Eur. J.* 2010, *16*, 12158-12167.

2 (a) Q. Zhou and T.M. Swager, *J. Am. Chem. Soc.*, 1995, **117**, 7017-7018; (a) Q. Zhou and T. M. Swager, *J. Am. Chem. Soc.*, 1995, **117**, 12593-12602.

3 (a) W. M. Ashton, *Nature*, 1972, **237**, 46-47; (b) C. Prophete, E. A. Carlson, Y. Li, J. Duffy, B. Steinetz, S. Lasano, J. T. Zelikoff, *Fish Shellfish Immunol.*, 2006, **21**, 325-334.

4 M. Dutta and D. Das, *Trend. Anal.Chem.*, 2012, **32**, 113-132.

5 (a) G. B. Li, H. C. Fang, Y. P. Cai, Z. Y. Zhou, P. K. Thallapally, and J. Tian, *Inorg. Chem.*, 2010, **49**, 7241-7243; (b) S. Ghosh, R. Chakrabarty and P. S. Mukherjee, *Inorg. Chem.*, 2009, **48**, 549-556; (c) H. Wang, D. Wang, Q. Wang, X. Li and C. A. Schalley, *Org. Biomol. Chem.*, 2010, **8**, 1017-1026; (d) N. Aksuner, E. Henden, I. Yilmaz and A. Cukurovali, *Sensor. Actuat. B Chem.*, 2012, **166-167**, 269-274; (e) W. Lin, L. Yuan, Z. Cao, J. Feng and Y. Feng, *Dyes Pigments*, **2009**, *83*, 14-20; (f) F. A. Abebe, C. S. Eribal, G. Ramakrishna and E. Sinn, *Tetrahedron Lett.*, 2011, **52**, 5554-5558; (g) S. Maisonneuve, Q. Fan and J. Xie, *Tetrahedron*, 2008, **64**, 8716-8720; (h) C. Ma, A. Lo, A. Abdolmaleki and M. J. MacLachlan, *Org. Lett.*, 2004, **6**, 3841-3844; (i) Y. D. Fernandez, A. P. Gramatges, V. Amendola, F. Foti, C. Mangano, P. Pallavicini and S. Patroni, *Chem. Commun.*, 2004, 1650-1651; (j) Y. Xiao and X. Qian, *Tetrahedron Lett.*, 2003, **44**, 2087-2091; (k) I. Grabchev, J. M. Chovelon and X. Qian, *New J. Chem.*, 2003, **27**, 337-340; (l) F. Bolletta, I. Costa, L. Fabbrizzi, M. Licchelli, M. Montalti, P. Pallavicini, L. Prodi and N. Zaccheroni, *J. Chem. Soc., Dalton Trans.*, 1999, 1381-1385; (m) N. Chattopadhyay, A. Mallick, S. Sengupta, *J. Photochem. Photobiol. A: Chemistry*, 2006, **177**, 55-60; (n) S. C. Dodani, Q. He, and C. J. Chang, *J. Am. Chem. Soc.*, 2009, **131**, 18020-18021.

6 (a) Y. Zhang, C. B. Murphy, W. E. Jones, *Macromolecules*, 2002, **35**, 630-636; (b) J. Feng, Y. Li, M. Yang, *J. Polym. Sci. Part A: Polym. Chem.*, 2009, **47**, 222-230; (c) Y. Liu, S. Zhang, Q. Miao, L. Zheng, L. Zong, Y. Cheng, *Macromolecules*, 2007, **40**, 4839-4847; (d) X. Huang, Y. Xu, Q. Miao, L. Zong, H. Hu, Y. Cheng, *Polymer*, 2009, **50**, 2793-2805; (e) X. Huang, Y. Dong, J. Meng, Y. Cheng, C. Zhu, *Synlett.*, 2010, **12**, 1841-1844.

7 (a) A. Qin, J. W. Y. Lam and B. Z. Tang, *Chem. Soc. Rev.*, 2010, **39**, 2522-2544; (b) A. Qin, J. W. Y. Lam and B. Z. Tang, *Macromolecules*, 2010, **43**, 8693-8702.

8 J. J. Bryant and U. H. F. Bunz, *Chem. Asian J.*, 2013, **8**, 1354-1367.

9 Y. H. Lau, P. J. Rutledge, M. Watkinson and M. H. Todd, *Chem. Soc. Rev.*, 2011, **40**, 2848-2866.

10 (a) Y. Wu, Y. Dong, J. Li, X. Huang, Y. Cheng, C. Zhu, *Chem. Asian J.*, 2011, **6**, 2725-2729; (b) L. Zheng, X. Huang, Y. Shen, Y. Cheng, *Synlett.*, 2010, 453-456.

11 (a) S. J. Liu, C. Fang, Q. Zhao, Q. L. Fan and W. Huang, *Macromol. Rapid. Commun.*, 2008, **29**, 1212-1215; (b) X. B. Huang, J. Meng, Y. Dong, Y. X. Cheng and C. J. Zhu, *J. Polym. Sci. Part A Polym. Chem.*, 2010, **48**, 997-1006; (c) X. B. Huang, Y. Xu, L. F. Zheng, J. Meng and Y. X. Cheng, *Polymer*, 2009, **50**, 5996-6000; (d) J. Li, J. Meng, X. B. Huang, Y. X. Cheng and C. J. Zhu, *Polymer*, 2010, **51**, 3425-3430; (e) X. Ma, F. Y. Song, L. Wang, Y. X. Cheng and C. J. Zhu, *J. Polym. Sci. Part A Polym. Chem.*, 2012, **50**, 517-522; (f) D. Q. Li, H. Li, M. C. Liu, J. X. Chen, J. C. Ding, X. B. Huang and H. Y. Wu, *Macromol. Chem. Phys.*, 2014, **215**, 82-89.

12 (a) R. Yang, R. Tian, W. Yang, Q. Hou and Y. Cao, *Macromolecules*, 2003, **36**, 7453-7460; (b) R. Yang, R. Tian, J. Yan, Y. Zhang, J. Yang, Q. Hou, W. Yang, C. Zhang and Y. Cao, *Macromolecules*, 2005, **38**, 244-253; (c) J. Hou, T. L. Chen, S. Zhang, H. Y. Chen and Y. Yang, *J. Phys. Chem. C*, 2009, **113**, 1601-1605; (d) J. Hou, M. H. Park, S. Zhang, Y. Yao, L. M. Chen, J. H. Li, Y. Yang, *Macromolecules*, 2008, **41**, 6012-6018; (e) T. Yasuda, T. Imase, T. Yamamoto, *Macromolecules*, 2005, **38**, 7378-7385; (f) J. Yang, C. Jiang, Y. Zhang, R. Yang, W. Yang, Q. Hou, Y. Cao, *Macromolecules*, 2004, **37**, 1211-1218; (g) S. Uchiyama, K. Kimura, C. Gota, K. Okabe, K. Kawamoto, N. Inada, T. Yoshihara and S. Tobita, *Chem. Eur. J.*, 2012, **18**, 9552-9563; (h) S. Das, P. B. Pati, S and S. Zade, *Macromolecules*, 2012, 45, 5410-5417; (i) M. İçli-Özkut, H. İpek, B. Karabay, A. Cihaner and A. M. Önal, *Polym. Chem.*, 2013, **4**, 2457-2463; (j) G. Qian, H. Abu and Z. Y. Wang, *J. Mater. Chem.*, 2011, **21**, 7678-7685; (k) F. B. Koyuncu, A. R. Davis and K. R. Carter, *Chem. Mater.*, 2012, **24**, 4410-4416; (l) G. L. Gibson, T. M. McCormick and D. S. Seferos, *J. Am. Chem. Soc.* 2012, **134**, 539-547; (m) L. Chen, L. Wang, X. Jing and F. Wang, *J. Mater. Chem.*, 2011, **21**, 10265-10267.

13 J. J. Bryant, B. D. Lindner and U. H. F. Bunz, *J. Org. Chem.*, 2013, **78**, 1038-1044.

14 S. J. Liu, Q. Zhao, R. F. Chen, Y. Deng, Q. L. Fan, F. Y. Li, L. H. Wang, C. H. Huang and W. Huang. *Chem. Eur. J.*, 2006, **12**, 4351-4361.

15 S. P. Dudek, M. Pouderoijen, R. Abbel, A. P. H. J. Schenning and E. W. Meijer, *J. Am. Chem. Soc.*, 2005, **127**, 11763-11768.

16 D. Li, X. Wang, Y. Jia, A. Wang, Y. Wu, *Chin. J. Chem.*, 2012, **30**, 861-868.
17 B. A. D. Neto, A. S. Lopes, G. Ebeling, R. S. Goncalves, V. E. U. Costa, F. H. Quina, J. Dupont, *Tetrahedron*, 2005, **61**, 10975-10982.
18 D. Q. Li, H. Li, M. C. Liu, J. X. Chen, J. C. Ding, X. B. Huang and H. Y. Wu, *Polymer*, 2013, **54**, 6158-6164.
19 V. V. Rostovtsev, L. G. Green, V. V. Fokin and K. B. Sharpless, *Angew. Chem. Int. Ed.*, 2002, **41**, 2596-2599.
20 W. Lin, L. Yuan, Z. Cao, J. Feng and Y. Feng. *Dyes Pigm.*, 2009, **83**, 14-20.
21 (a) H. A. Benesi and J. H. Hildebrand, *J. Am. Chem. Soc.*, 1949, **71**, 2703-2707; (b) J. Wen, L. Dong, J. Tian, T. Jiang, Y. Q. Yang, Z. Huang, X. Q. Yu, C. W. Hu, S. Hu, T. Z. Yang and X. L. Wang, *J. Hazard. Mater.*, 2013, **263**, 638-642; (c) Y. Zhang, G. Wang and J. Zhang, *Sensor. Actuat. B Chem.*, 2014, **200**, 259-268; (d) Z. H. Xu, L. Zhang, R. Guo, T. Xiang, C. Wu, Z. Zheng and F. Yang, *Sensor. Actuat. B Chem.*, 2011, **156**, 546-552; (e) S. R. Liu and S. P. Wu, *J. Fluoresc.*, 2011, **21**, 1599-1605.

Highly sensitive conjugated polymer fluorescent sensors based on benzochalcogendiazole for nickel ions in real-time detection

Yunxiang Lei, Hui Li, Wenxia Gao, Miaochang Liu, Jiuxi Chen, Jinchang Ding, Xiaobo Huang and Huayue Wu

Two conjugated polymer fluorescent sensors **P-1** and **P-2** using a benzochalcogendiazole unit and a triazole unit as cooperative receptors were synthesized by the CuAAC reaction. Compared with benzothiadiazole-based **P-2**, benzoselenadiazole-based **P-1** showed higher sensitivity and selectivity because of the specific electronegativity of selenium. The quenching of **P-1** fluorescence gave a linear response toward Ni^{2+} in the range of 0–1.8 μmol·L^{-1}, with a detection limit of 2.4 nM.